CrystEngComm

Accepted Manuscript

ROYAL SOCIETY OF CHEMISTRY

www.rsc.org/crystengcomm

Journal Name

RSCPublishing

ARTICLE

Anions-Templated Assembly of Three Indium-Organic Frameworks with Diverse Topologies

Cite this: DOI: 10.1039/x0xx00000x

Jing Wang, Jiahuan Luo, Bo Zhi, Guanghua Li, Qisheng Huo and Yunling Liu*

Received 00th January 2012,
Accepted 00th January 2012

DOI: 10.1039/x0xx00000x

www.rsc.org/

$[In(bpydc)(NO_3)(DMA)_{0.5}]\cdot(DMA)(H_2O)_{4.5}$ (**JLU-Liu8**), $[In(bpydc)(HCOO)H_2O]\cdot(DMF)_2(H_2O)_3$ (**JLU-Liu9**) and $[In(bpydc)Cl]\cdot(DMF)_2(H_2O)_3$ (**JLU-Liu10**), three novel 3D monoatomic indium-organic frameworks, have been synthesized by 2,2′-bipyridyl-5,5′-dicarboxylic acid (H_2bpydc) ligand under solvothermal conditions. These three compounds are constructed by the same ligand, but templated by three different anions (NO_3^-, $HCOO^-$ and Cl^-), and they exhibit three different 4-connected **ung**, **crb** and **cbo** network topologies. **JLU-Liu8** exhibits two types of single-helical chains with opposite helical directions (left-handed and right-handed), all of the left-handed and right-handed helical chains alternate together. In the structure of **JLU-Liu9**, there are two types of metal-ligand channels: the smaller square channels with dimensions 3.45 × 4.03 Å and the bigger square channels with dimensions 11.5 × 11.5 Å. **JLU-Liu10** displays interesting feature of double-helical chains: both of the helical chains are interconnected with each other by sharing indium ions which entangles one spiral shafts. Furthermore, the role of anions in assisting the formation of distinct structures has been discussed. These three compounds display strong luminescence in the solid state at room temperature.

Introduction

Metal-organic frameworks (MOFs) have attracted much attention due to their structural diversity and tailorability,[1] as well as potential applications in the fields of gas adsorption and separation,[2] catalysis,[3] luminescence,[4] magnetism[5] and drug delivery.[6] Organic linkers as the component play vital roles not only in the construction but also in the functions, and unique properties can be designed and fine-tuned through the judicious choice of organic ligands. Among the numerous ligands, the multidentate ligands with hybrid oxygen-nitrogen donors, which provide different functional sites, have been often explored to assemble of MOFs. 2,2'-bipyridyl-5,5′-dicarboxylic acid (H_2bpydc),[7] as a heterocyclic carboxylate ligand with coordinated nitrogen and oxygen atoms, has been explored. The H_2bpydc ligand exhibits two main coordinated modes: one is in the linear mode with two nitrogen donors of the 2,2'-bipyrine group open or loaded metal ions such as Pd, Ir, Ru and Cu ions, and the other is in the T-shaped mode with all coordination sites linked with metal centers. MOFs based on the H_2bpydc ligand with different metals exhibit fascinating structures and multiple properties. For instance, Yaghi's group utilized the H_2bpydc ligand to synthesize a microporous MOF with open nitrogen atom sites, which functionalized by Pd^{2+} and Cu^{2+}, and lead to a significantly enhanced selectivity for the adsorption of CO_2 over N_2.[7a] Lin and co-workers reported a series of highly stable MOFs materials with functionalized H_2bpydc ligand, and exhibited high catalysis activities.[7f,g] In addition, our group synthesized two flexible MOFs by H_2bpydc ligand and transition metals which exhibited uncommon stepwise N_2 and CO_2 adsorption behaviors.[7h] Therefore, H_2bpydc ligand is a promising candidate for the construction of functional MOFs with different properties.

Recently, our group, among others, is focused on the design and synthesis of indium based MOFs (In-MOFs).[8] Compared to other p-block metals, indium ions are known to form monomers, dimers, chains and trimers secondary building units, when they coordinate to different organic ligands, the constructed In-MOFs display diverse topological structures and remarkable gas storage, catalytic and fluorescence properties.[8, 9]

As a continuation of our previous work, herein, we selected indium as metal source, and successfully synthesized three novel In-MOFs with H_2bpydc ligands, namely $[In(bpydc)(NO_3)(DMA)_{0.5}]\cdot(DMA)(H_2O)_{4.5}$ (**JLU-Liu8**), $[In(bpydc)(HCOO)H_2O]\cdot(DMF)_2(H_2O)_3$ (**JLU-Liu9**) and $[In(bpydc)Cl]\cdot(DMF)_2(H_2O)_3$ (**JLU-Liu10**), which exhibited rarely 4-connected **ung**, **crb** and **cbo** topologies, respectively. Generally, several synthetic factors of MOFs can effectively alter the topology of coordination assemblies, such as the metal/ligand ratio, the reaction solvent system, temperature and templates. Thus, considerable efforts have been devoted to design synthetic conditions according to these factors. The structures, luminescent properties, infrared spectra (IR), elemental analyses, powder X-ray diffraction (PXRD), and thermogravimetric (TGA) analyses were carried out in detail. Furthermore, the influence of different coordinated anions in the construction of the three compounds was discussed.

Experimental

Materials and methods

All chemicals were obtained from commercial sources and used without further purification. Powder X-ray diffraction (XRD) data were collected on a Rigaku D/max-2550 diffractometer with Cu Kα radiation (λ = 1.5418 Å). Elemental analyses (C, H, and N) were achieved by vario MICRO (Elementar, Germany). Thermogravimetric analyses (TGA) were detected on a TGA Q500 thermogravimetric analyzer (TA, America) in the temperature range of 35-800^{o}C under air flow with the heating rate of 10 ^{o}C min^{-1}. Fourier transform infrared (IR) measurements were recorded within the 400-4000 cm^{-1} region on an IFS-66V/S IR spectrometer (Bruker, Germany). The fluorescence spectra were detected by a FLUOROMAX-4 (HORIBA Jobin Yvon, America) series spectrofluorometer at room temperature.

Synthesis of JLU-Liu8

A mixture of $In(NO_3)_3{\cdot}4H_2O$ (0.008 g, 0.022 mmol), 2,2′-bipyridyl-5,5′-dicarboxylic acid (0.008 g, 0.033 mmol), HNO_3 (0.1 mL, 2.8 M in DMF), and 1 mL of DMA was sealed into a 20 mL vial and heated at 85 °C for 12 h and 105 °C for another 4h. Eventually, the mixture was cooled to room temperature, after which colorless crystals were collected and dried in the air (65% yield based on $In(NO_3)_3{\cdot}4H_2O$). Elemental analysis (wt %) for **JLU-Liu8**: Calcd: C 34.27, H 4.554, N 9.992%. Found: C 34.55, H 4.661, N 10.97%. FT-IR (KBr, cm^{-1}): 3052(w), 2937(w), 1649(s), 1489(m),1347(s), 1159(m), 1034(m), 852(m), 776(s).

Synthesis of JLU-Liu9

A mixture of $In(NO_3)_3{\cdot}4H_2O$ (0.010 g, 0.03 mmol), 2,2′-bipyridyl-5,5′-dicarboxylic acid (0.003 g, 0.01 mmol), 0.08 mL HCOOH, 1 mL of DMF and 0.5 mL of DEF was sealed into a 20 mL vial and heated at 105 °C for 4d. Eventually, the mixture was cooled to room temperature, after which yellow crystals were collected and dried in the air (61% yield based on $In(NO_3)_3{\cdot}4H_2O$). Elemental analysis (wt %) for **JLU-Liu9**. Calcd: C 36.79, H 4.712, N 9.032%. Found: C 36.88, H 4.911, N 9.194%. FT-IR (KBr, cm^{-1}): 3057(w), 2932(w), 1640(s), 1342(s), 1151(w), 1034(m), 847(m), 776(s).

Synthesis of JLU-Liu10

A mixture of $InCl_3{\cdot}4H_2O$ (0.005 g, 0.02 mmol), 2,2′-bipyridyl-5,5′-dicarboxylic acid (0.005 g, 0.02 mmol), 1mL of DMF was sealed into a 20 mL vial and heated at 85 °C for 15 h. Eventually, the mixture was cooled to room temperature, after which yellow crystals were collected and dried in the air (57% yield based on $InCl_3{\cdot}4H_2O$). Elemental analysis (wt %) for **JLU-Liu10**. Calcd: C 36.47, H 4.421, N 9.453%. Found: C 36.79，H 4.633，N 9.512%. FT-IR (KBr, cm^{-1}): 3057(w), 2928(w), 1649(s), 1373(s), 1155(m), 1039(m), 839(m), 776(s).

The phase purity of as-synthesized samples was confirmed by the evident similarities between the calculated and the experimental PXRD patterns (see the ESI† Fig. S4). The IR spectra for compounds are shown in ESI Fig. S5.

X-ray Crystallography

Crystallographic data for **JLU-Liu8-10** were collected on a Bruker Apex II CCD diffractometer using graphite-monochromated Mo-*K*α (λ = 0.71073 Å) radiation at room temperature. The structures were solved by direct methods and refined by full-matrix least-squares on F^2 using SHELXTL Version 5.1.[10] All the metal atoms were located first, and then the oxygen and carbon atoms of the compounds were

Table 1 Crystal data and structure refinement for **JLU-Liu8**, **JLU-Liu9** and **JLU-Liu10**

compound	**JLU-Liu8**	**JLU-Liu9**	**JLU-Liu10**
formula	$C_{18}H_{28.5}InN_{4.5}O_{13}$	$C_{19}H_{29}InN_4O_{12}S_2$	$C_{18}H_{26}ClInN_4O_9$
fw	630.77	620.28	592.70
temp (K)	296(2)	293(2)	293(2)
crystal system	trigonal	tetragonal	cubic
space group	*R3c*	*I-4*	*Pa-3*
a (Å)	31.4162(16)	24.681(4)	27.590(3)
b (Å)	31.4162(16)	24.681(4)	27.590(3)
c (Å)	14.1226(14)	10.819(2)	27.590(3)
α (deg)	90	90	90
β (deg)	90	90	90
γ (deg)	120	90	90
V (Å^3)	12071.3(15)	6590.7(19)	21002(4)
Z	18	8	24
Dc (Mg/m^3)	1.562	1.250	1.125
μ(mm^{-1})	0.949	0.769	0.789
F(000)	5778	2528	7200
reflections collected	22769/5637	21407/6051	114483/7165
unique (Rint)	0.0261	0.0507	0.0400
GOF on F^2	1.040	1.083	1.169
R1, wR2 [I>2σ(I)]	0.0461, 0.1256	0.0702, 0.1936	0.0510, 0.1656
R1, wR2 (all data)	0.0500, 0.1307	0.0753, 0.1970	0.0677, 0.1717

$R_1 = \sum||F_o|-|F_c||/\sum|F_o|$. $wR_2 = [\sum[w(F_o^2-F_c^2)^2]/\sum[w(F_o^2)^2]]^{1/2}$

subsequently found in difference Fourier maps. The hydrogen atoms of the ligand were placed geometrically. All non-hydrogen atoms were refined anisotropically. The final formulas were derived from crystallographic data combined with elemental and thermogravimetric analysis data. Crystallographic data for **JLU-Liu8-10** (1002212-1002214) have been deposited with Cambridge Crystallographic Data Centre. Data can be obtained free of charge upon request at www.ccdc.cam.ac.uk/data_request/cif. Crystal data and detailed data collection and refinement of **JLU-Liu8-10** are summarized in Table 1. Topology information for the three compounds were calculated by TOPOS 4.0.[11]

Results and discussion

Structure description of compound JLU-Liu8

Single-crystal X-ray diffraction analysis reveals that compound **JLU-Liu8** crystallizes in the trigonal crystal system with space group of *R3c*. The asymmetric unit of compound **JLU-Liu8** consists of one indium atom, one ligand molecule, half of DMA molecule and one NO_3^- anion (Fig. 1a). The indium atom displays decahedral $[InN_2O_5]$ geometry[12] with two nitrogen and two oxygen atoms from three individual ligands, one oxygen atom from DMA, two oxygen atoms from NO_3^- (Fig. S1a†). The In-O and In-N bond distance is in the range of 2.095-2.505 Å and 2.276-2.284 Å, respectively. The H_2bpydc ligand is deprotonated to be bpydc^{2-} and adopts monodentate bridging coordination mode, which offers two oxygen and two nitrogen atoms to coordinate with three indium atoms as shown in Scheme 2f. In **JLU-Liu8**, each indium ion connects with three ligands to form a 3D framework (Fig. S1b†), in which there are two types of channels along the *c* axis. The large channel is surrounded by the six small channels (Fig. 1b). Interestingly, each small channel is made up of left- and right-handed helical chains, and the left- and right-handed helical chains exist alternately. Both helical channels can be viewed as $\{In^{III}\ldots In^{III}\ldots In^{III}\}$ centers arranged in clockwise / anticlockwise direction with 88.1° span to generate two helical chains with a pitch of 14.1 Å (Fig. 1c). All two adjacent helical chains are bridged by sharing partial H_2bpydc ligands. The partial H_2bpydc ligands are bound to indium ions to form a zigzag chain between two helical chains along the *c* axis (Fig. 1d). Then, six zigzag chains interconnect with six helical chains to form a large 1D channel of 11.7 × 11.7 Å (Fig. 1e, S1c†). Topologically, each indium ion linked to other four surrounding indium ions through the bridging bpydc^{2-} ligands, and can be regarded as a 4-conneced tetrahedral node. The 3D framework can be simplified as a tetrahedral network with **ung** topology (Fig. 1f, S1e†). PLATON[13] analysis reveals that the 3D porous structure is composed of solvent area volume of 7027.2 Å^3, which represents 58.2% per unit cell volume.

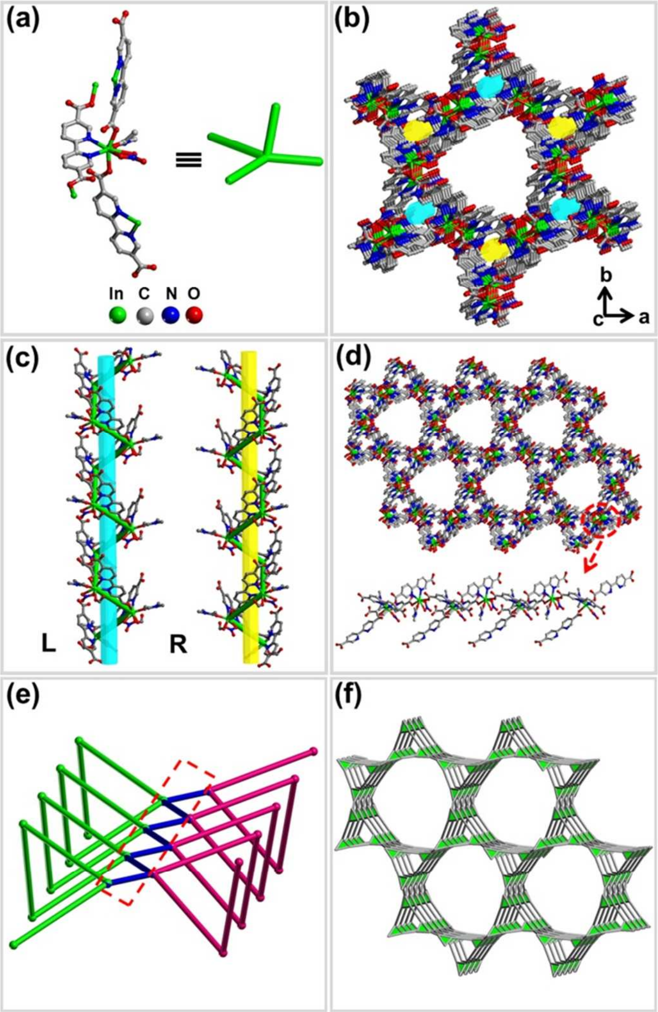

Fig. 1 A description of the structure for **JLU-Liu8**: (a) the coordination environment of the In^{3+} ions; (b) view of channels with helical chains along the *c* axis; (c) two types of helical chains (left-handed and right-handed); (d) zigzag chains along the *c* axis; (e) six zigzag chains are bound to six helical chains to form a big 1D channel of 11.7 Å; (f) topological features of **JLU-Liu8**.

Structure description of JLU-Liu9

Single-crystal X-ray diffraction analysis reveals that **JLU-Liu9** crystallizes in the tetragonal crystal system with space group of *I-4*. The asymmetric unit of **JLU-Liu9** consists of one crystallographically independent indium atom, one ligand, one formic acid molecule and one water molecule (Fig. 2a). The indium atom displays octahedral $[InN_2O_4]$ geometry, in which two nitrogen atoms are from one ligand, two oxygen atoms are from two distinct ligands and the other two oxygen atoms are from water molecule and formic acid molecule (Fig. S2a†). The In-O bond distance lies in the range of 2.094-2.149 Å and In-N bond distance lies in the range of 2.261-2.286 Å. The deprotonated H_2bpydc ligand also adopts monodentate bridging coordination mode, which offers two oxygen and two nitrogen atoms to coordinate with three indium atoms as shown in Scheme 2g. In the structure of **JLU-Liu9**, there exist two types of metal-ligand channels; the smaller square channel is surrounded by four bigger square channels (Fig. S2c†). The dimensions of the smaller and bigger channels are about 4.9 × 4.9 Å and 11.5 × 11.5 Å with the terminal water molecules omitted (Fig. 2b, 2c). Then, the two types of channels are

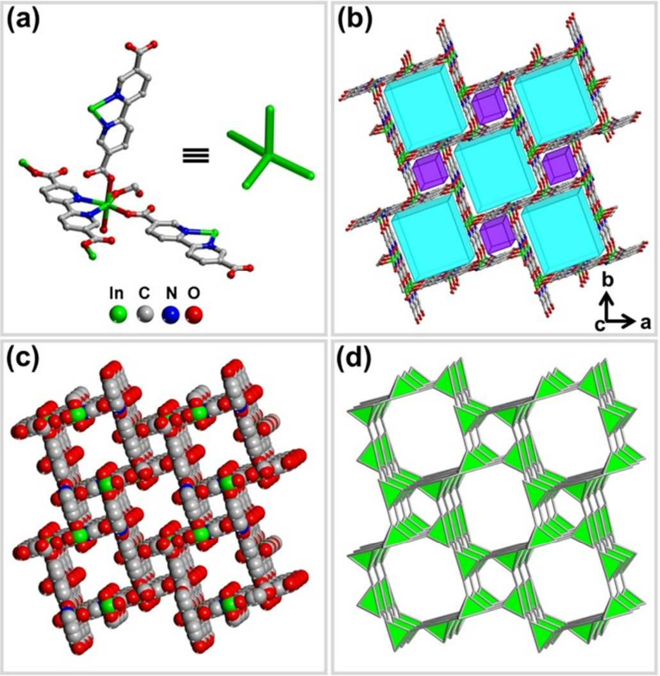

Fig. 2 A description of the structure for **JLU-Liu9**: (a) illustration of the In^{3+} ions; (b) ball and stick model of the 3D framework along the *c* axis; (c) two kinds of channels; (d) topological features of **JLU-Liu9**.

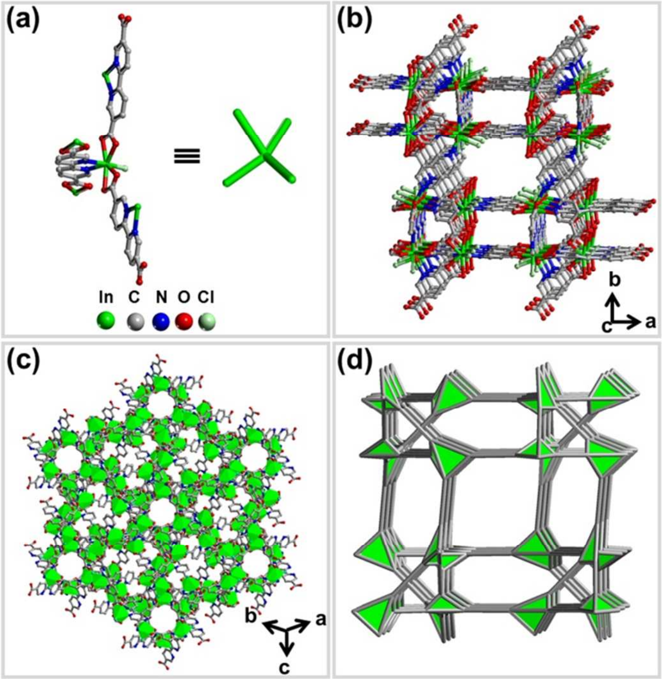

Fig. 3 A description of the structure for **JLU-Liu10**: (a) illustration of the In^{3+} ions; (b) ball and stick model of the 3D framework; (c) the polyhedron of the compound along [111] direction; (d) topological features of **JLU-Liu10**.

arranged alternatively to form a 3D framework with the Reticular Chemistry Structure Resource (RCSR) code **crb**,[14] which can be referred to as a zeolitic topology **BCT**[15] (Fig. 2d, S2d†). PLATON analysis reveals that the 3D porous structure is composed of solvent area volume of 4410.2 Å^3, which represents 66.9% per unit cell volume.

Structure description of JLU-Liu10

Single-crystal X-ray diffraction analysis reveals that compound **JLU-Liu10** crystallizes in the cubic crystal system with space group of *Pa-3*. The asymmetric unit of compound **JLU-Liu10** consists of one indium atom, one ligand, and one terminal chloride ion (Fig. 3a). The indium ion displays decahedral $[InN_2O_4Cl]$ geometry[12], in which two nitrogen atoms are from one ligand, four oxygen atoms are from two distinct ligands and one chloride atom (Fig. S3a†). The In-O and In-N bond distance lie in the range of 2.185-2.459 Å and 2.247-2.266 Å, respectively. The deprotonated H_2bpydc ligand adopts bidentate bridging coordination mode, which offers four oxygen and two nitrogen atoms to coordinate with three indium atoms as shown in Scheme 2h. In compound **JLU-Liu10**, indium ions connected to the organic ligands to generate a 3D framework (Fig. 3b). The most interesting feature of the structure is there existing double-helical chains along the [111] direction (Fig. 3c). Each double-helical chain is made up of left- handed and right-handed helical chains, both of them are interconnected with each other by sharing indium ions entangling one spiral shafts. There are two types of double-helical chains (Fig. 4), which are bridged by sharing partial bpydc^{2-} ligands. The two types of helical chains connect with each other alternately to give rise to a 3D framework, in which there is a big channel with diameter about 11 × 11 Å (Fig. S3c†). Similarly to **JLU-Liu8** and **JLU-Liu9**, the indium ion in **JLU-Liu10** can be regarded as a 4-connected tetrahedral node, but arranged in a different symmetry, then generate a 4-connected net with **cbo** topology (Fig. S3d†). PLATON analysis reveals that the 3D porous structure is composed of solvent area volume of 15462 Å^3, which represents 73.6% per unit cell volume.

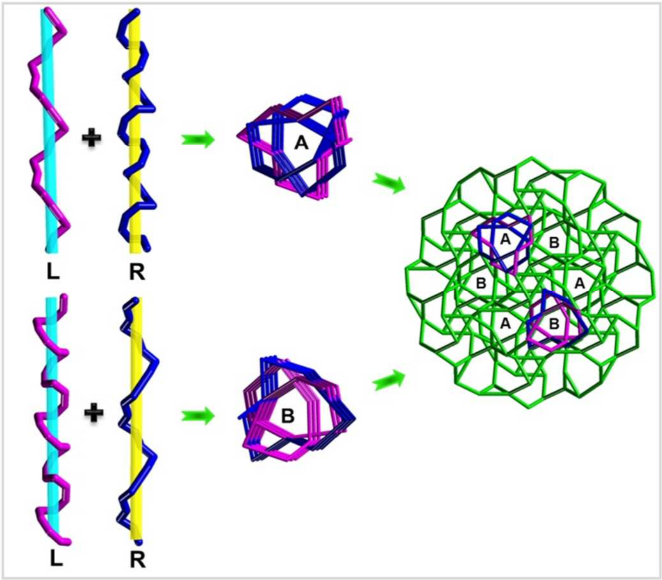

Fig. 4 Double-helical chains along the [111] direction.

JLU-Liu8, **JLU-Liu9** and **JLU-Liu10** are solvent exchanged and activated. The TGA curves show that guest molecules have been successful exchanged. However, the XRPD indicates that the frameworks of all the compounds can't maintain their crystallinity upon immersing the samples in common solvents such as acetonitrile, chloroform, acetone, dichloromethane and ethanol. N_2 adsorption studies indicate that these compounds show very little N_2 adsorption.

It is well known that the experimental synthesis parameters such as metal, ligand, solvent, pH value, temperature, as well as cationic species,[16a] and organic templates,[16b,c,d] may affect the final structures, nevertheless the importance of anionic templates for the construction of MOFs is comparatively less explored. The anions can dictate assembly by either coordinating strongly to the vacant sites on the metal center, or remaining as non-coordinating counterions in the channels.[17] For example, Cheng and co-workers reported two novel Dy-Cu MOFs, in which the coordinated anions induced change of structure interpenetration and magnetic properties.[17a] Thus, design and choice of different geometric anions are crucial to construct novel frameworks. In this paper, we have synthesized three novel In-MOFs assisting by different geometric anions such as NO_3^-, $HCOO^-$ and Cl^-. Although all of the In-MOFs display 4-connected tetrahedral nodes, the angles of tetrahedron are quite different in the simplified structures (Fig. S7†). Due to the steric effect of the terminal coordinate anions, the three In-MOFs exhibit 4-conected topologies and avoid the formation of the default diamond structure.[18] Up to now, more than 30 kinds of zeolite topologies of zeolite-like MOFs have been synthesized by using different synthesis strategies,[8a,c, 19] anions-templated synthesis method we report here, will be an effective strategy to generate MOFs with zeolite topologies, such as **JLU-Liu9**. The coordination modes of anions (NO_3^-, $HCOO^-$ and Cl^-) in the construction of In-MOFs have been shown in Scheme 1. The role of anion may be explained as followings: (1) attainment of charge equilibrium of the framework; (2) steric effect; (3) templates/structure directing agent. Therefore, anion plays important roles in exploring the novel structure.

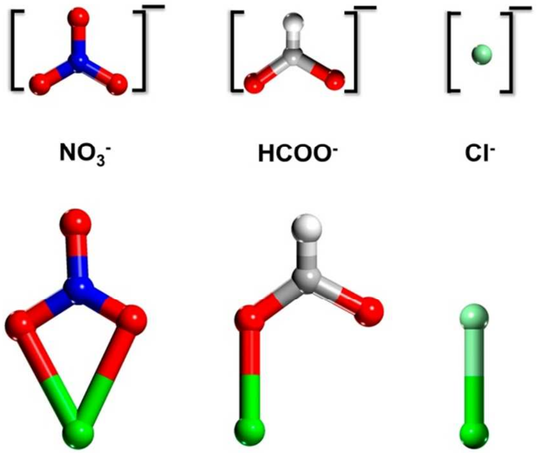

Scheme 1. Coordination modes for anions. Color scheme: metal, green.

A study of H_2bpydc ligand based MOFs indicate that eleven types of coordination modes have been given (Scheme 2), and five coordination modes (Scheme 2a-e) have been reported in the literature. It is found that all or part of the oxygen/nitrogen atoms of H_2bpydc ligand display strong chelating ability. More coordination modes of H_2bpydc ligand will be adequately discovered by the reasonable selection of metal ions. Indium ion with 6-8 coordination numbers is known for its monoatomic, dimeric and trimeric inorganic building units, therefore it is a good choice for construction of MOFs with H_2bpydc ligand. As expectation, three novel coordination modes (f)-(h) have been explored in this paper. Because of the varieties of coordination modes of H_2bpydc ligand, **JLU-Liu8**, **JLU-Liu9** and **JLU-Liu10** exhibit diverse structures. Some new coordination modes (Scheme 2i-k) may be found in the future.

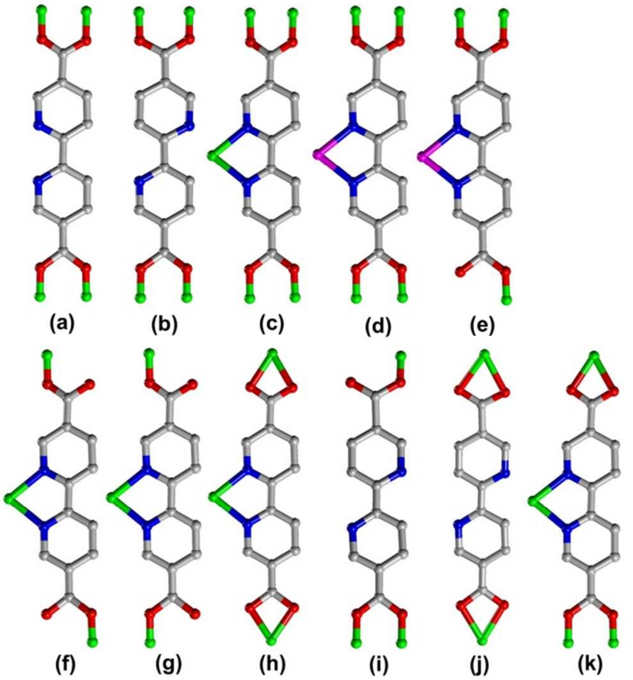

Scheme 2. Coordination modes for H_2bpydc. Color scheme: carbon, gray; nitrogen, blue; oxygen, red; metal, green and pink.

Thermogravimetric Analysis

As shown in Fig. S6†, TG analysis for **JLU-Liu8** shows a weight loss of 35 % between 30 and 300°C, which corresponds to the loss of the DMA and H_2O molecules. Upon further heating, a weight loss of 44 % between 300 and 500°C occurs due to the collapse of the framework (calcd: 47%). PXRD studies indicated that the final product, upon calcinations above 500°C, is a main phase of In_2O_3 (JCPDS: 71-2194).

TG analysis for **JLU-Liu9** shows a weight loss of 30 % between 30 and 300°C, which corresponds to the loss of H_2O molecules and DMF molecules. Upon further heating, a weight loss of 44% between 300 and 550°C occurs due to the collapse of the framework (calcd: 45 %). PXRD studies indicated that the final product, upon calcinations above 550°C, is a main phase of In_2O_3 (JCPDS: 71-2194).

TG analysis for **JLU-Liu10** shows a weight loss of 39 % between 30 and 400°C, which corresponds to the loss of H_2O and DMF molecules. Upon further heating, a weight loss of 38% between 400 and 650°C occurs due to the collapse of the framework (calcd: 39 %). PXRD studies indicated that the final product, upon calcinations above 600°C, is a main phase of In_2O_3 (JCPDS: 71-2194).

Luminescence Properties

Luminescence compounds had attracted intense interest due to their potential applications, such as in photochemistry, chemical sensors, electroluminescent displays, and so on. Indium based MOFs exhibited good luminescence properties.[20] The luminescence properties of the three as-synthesized compounds and H_2bpydc ligand were evaluated in the solid state upon the excitation of 397 nm at room temperature (Fig. S8†). As shown in Fig. 5, the ligand showed two intense emission bands at 459 nm and 555 nm, respectively. **JLU-Liu8**, **JLU-Liu9** and **JLU-Liu10** exhibited intensive blue luminescence emission maximum at 473 nm, 490 nm and 479 nm, a little shift from the H_2bpydc ligand, which could be attributed to the π→π* charge transition within the aromatic rings of the ligand. The disappearances of the excimer peak of the ligand (at 555 nm) and the vibronic peaks around 459 nm could be due to the loss of the interaction between the ligands and the ring vibrations of the ligands after forming the 3D framework. The strong intensity of compounds might be due to the interaction between H_2bpydc ligand and the In^{3+} ion, which increased the rigidity of ligand and reduced the non-radioactive loss.[21]

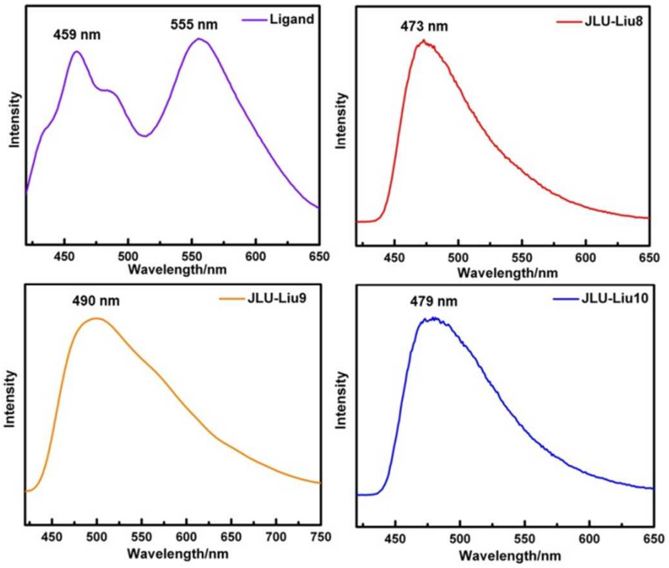

Fig. 5 Luminescent spectra of H_2bpydc ligand and three compounds at room temperature.

Conclusions

In summary, we use H_2bpydc ligand to react with different In(III) sources to construct three novel monomeric MOFs under varied solvothermal conditions. These three In-MOFs are obtained by the assistance of different geometric anions such as NO_3^-, $HCOO^-$ and Cl^-, and the employment of different anions leads to diverse structures with different 4-connected **ung**, **crb** and **cbo** network topologies. The structural feature of **JLU-Liu8** is the single-helical chain, which exhibits two types of helical channels with opposite helical chains. In the structure of **JLU-Liu9**, there are two kinds of metal-ligand channels: the smaller square channels and the bigger square channels. And **JLU-Liu10** shows interesting feature of double-helical chains. These results illustrate the significant role of anions in the formation of different novel frameworks. In addition, the luminescence properties of three compounds at room temperature are explored, and the results suggest that compounds exhibit good luminescence properties. Further properties research is ongoing in our group.

Acknowledgements

The authors gratefully acknowledge the financial support of the Natural Science Foundation of China (Grant Nos. 21373095, 21371067 and 21171064).

Notes and references

State Key Laboratory of Inorganic Synthesis and Preparative Chemistry, College of Chemistry, Jilin University, Changchun 130012, P. R. China. E-mail: yunling@jlu.edu.cn; Fax: +86-431-85168624.

†Electronic Supplementary Information (ESI) available: Selected bond lengths and angles, hydrogen bonding, additional figures for crystal structures, PXRD, IR and TGA. CCDC 1002212-1002214. For ESI and crystallographic data in CIF or other electronic format see DOI: 10.1039/b000000x

1 (*a*) P. Horcajada, R. Gref, T. Baati, P. K. Allan, G. Maurin, P. Couvreur, G. Férey, R. E. Morris and C. Serre, *Chem. Rev.*, 2012, **112**, 1232-1268; (*b*) J.-R. Li, J. Sculley and H.-C. Zhou, *Chem. Rev.*, 2012, **112**, 869-932; (*c*) H.-C. Zhou, J. R. Long and O. M. Yaghi, *Chem. Rev.*, 2012, **112**, 673-674; (*d*) Q. Lin, X. Bu and P. Feng, *Cryst. Growth Des.*, 2013, **13**, 5175-5178; (*e*) D.-X. Xue, A. J. Cairns, Y. Belmabkhout, L. Wojtas, Y. Liu, M. H. Alkordi and M. Eddaoudi, *J. Am. Chem. Soc.*, 2013, **135**, 7660-7667; (*f*) Z. R. Herm, B. M. Wiers, J. A. Mason, J. M. van Baten, M. R. Hudson, P. Zajdel, C. M. Brown, N. Masciocchi, R. Krishna and J. R. Long, *Science*, 2013, **340**, 960-964. (*g*) M. Zhang, Q. Wang, Z. Lu, H. Liu, W. Liu and J. Bai, *CrystEngComm*, 2014, **16**, 6287-6290; (*h*) Y.-S. Wei, R.-B. Lin, P. Wang, P.-Q. Liao, C.-T. He, W. Xue, L. Hou, W.-X. Zhang, J.-P. Zhang and X.-M. Chen, *CrystEngComm*, 2014, **16**, 6325-6330; (*i*) L. Li, J. Luo, S. Wang, Z. Sun, T. Chen and M. Hong, *Cryst. Growth Des.*, 2011, **11**, 3744-3747; (*j*) T.-H. Park, K. Koh, A. G. Wong-Foy and A. J. Matzger, *Cryst. Growth Des.*, 2011, **11**, 2059-2063.

2 (*a*) Y.-S. Bae and R. Q. Snurr, *Angew. Chem., Int. Ed.*, 2011, **50**, 11586-11596; (*b*) M. C. Das, Q. Guo, Y. He, J. Kim, C.-G. Zhao, K. Hong, S. Xiang, Z. Zhang, K. M. Thomas, R. Krishna and B. Chen, *J. Am. Chem. Soc.*, 2012, **134**, 8703-8710; (*c*) L. Du, Z. Lu, K. Zheng, J. Wang, X. Zheng, Y. Pan, X. You and J. Bai, *J. Am. Chem.*

Soc., 2012, **135**, 562-565; (*d*) J. Luo, J. Wang, G. Li, Q. Huo and Y. Liu, *Chem. Commun*., 2013, **49**, 11433-11435; (*e*) I. Spanopoulos, P. Xydias, C. D. Malliakas and P. N. Trikalitis, *Inorg. Chem*., 2013, **52**, 855-862.

3 (*a*) D. Farrusseng, S. Aguado and C. Pinel, *Angew. Chem., Int. Ed*., 2009, **48**, 7502-7513; (*b*) K. K. Tanabe and S. M. Cohen, *Inorg. Chem*., 2010, **49**, 6766-6774; (*c*) L. Bromberg, X. Su and T. A. Hatton, *Chem. Mater*., 2013, **25**, 1636-1642; (*d*) A. E. Platero-Prats, N. Snejko, M. Iglesias, Á. Monge and E. Gutiérrez-Puebla, E. *Chem.–Eur. J*., 2013, **19**, 15572-15582.

4 (*a*) A. Lan, K. Li, H. Wu, D. H. Olson, T. J. Emge, W. Ki, M. Hong and J. Li, *Angew. Chem., Int. Ed*., 2009, **48**, 2334-2338; (*b*) C. Y. Lee, O. K. Farha, B. J. Hong, A. A. Sarjeant, S. T. Nguyen and J. T. Hupp, *J. Am. Chem. Soc*., 2011, **133**, 15858-15861; (*c*) N. B. Shustova, A. F. Cozzolino and M. Dincă, *J. Am. Chem. Soc*., 2012, **134**, 19596-19599; (*d*) L.-N. Jia, L. Hou, L. Wei, X.-J. Jing, B. Liu, Y.-Y. Wang and Q.-Z. Shi, *Cryst. Growth Des*., 2013, **13**, 1570-1576; (*e*) X.-L. Qi, S.-Y. Liu, R.-B. Lin, P.-Q. Liao, J.-W. Ye, Z. Lai, Y. Guan, X.-N. Cheng, J.-P. Zhang and X.-M. Chen, *Chem. Commun*., 2013, **49**, 6864-6866.

5 (*a*) D. Sarma, K. V. Ramanujachary, S. E. Lofland, T. Magdaleno and S. Natarajan, *Inorg. Chem*., 2009, **48**, 11660-11676 (*b*) Y. Liu, H. Li, Y. Han, X. Lv, H. Hou and Y. Fan, *Cryst. Growth Des*., 2012, **12**, 3505-3513; (*c*) Z. Yan, M. Li, H.-L. Gao, X.-C. Huang and D. Li, *Chem. Commun*., 2012, **48**, 3960-3962.

6 S. R. Miller, D. Heurtaux, T. Baati, P. Horcajada, J.-M. Greneche and C. Serre, *Chem. Commun*., 2010, **46**, 4526-4528.

7 (*a*) E. D. Bloch, D. Britt, C. Lee, C. J. Doonan, F. J. Uribe-Romo, H. Furukawa, J. R. Long and O. M. Yaghi, *J. Am. Chem. Soc*., 2010, **132**, 14382-14384; (*b*) S. Huh, S. Jung, Y. Kim, S.-J. Kim and S. Park, *Dalton Trans*., 2010, **39**, 1261-1265; (*c*) M. Gustafsson, J. Su, H. Yue, Q. Yao and X. Zou, *Cryst. Growth Des*., 2012, **12**, 3243-3249; (*d*) C. A. Kent, D. Liu, T. J. Meyer and W. Lin, *J. Am. Chem. Soc*., 2012, **134**, 3991-3994; (*e*) L. Shen, D. Gray, R. I. Masel and G. S. Girolami, *CrystEngComm*, 2012, **14**, 5145-5147; (*f*) C. Wang, K. E. deKrafft and W. Lin, *J. Am. Chem. Soc*., 2012, **134**, 7211-7214; (*g*) C. Wang, Z. Xie, K. E. deKrafft and W. Lin, *J. Am. Chem. Soc*., 2011, **133**, 13445-13454; (*h*) J. Wang, J. Luo, J. Zhao, D.-S. Li, G. Li, Q. Huo and Y. Liu, *Cryst. Growth Des*., 2014, **14**, 2375-2380.

8 (*a*) Y. Liu, J. F. Eubank, A. J. Cairns, J. Eckert, V. C. Kravtsov, R. Luebke and M. Eddaoudi, *Angew. Chem., Int. Ed*., 2007, **46**, 3278-3283; (*b*) S. Wang, T. Zhao, G. Li, L. Wojtas, Q. Huo, M. Eddaoudi and Y. Liu, *J. Am. Chem. Soc*., 2010, **132**, 18038-18041; (*c*) Y. Liu, V. C. Kravtsov, R. Larsen and M. Eddaoudi, *Chem. Commun*., 2006, 1488-1490.

9 (*a*) X. Gu, Z.-H. Lu and Q. Xu, *Chem. Commun*., 2010, **46**, 7400-7402; (*b*) S.-T. Zheng, J. T. Bu, Y. Li, T. Wu, F. Zuo, P. Feng and X. Bu, *J. Am. Chem. Soc*., 2010, **132**, 17062-17064; (*c*) S.-T. Zheng, J. J. Bu, T. Wu, C. Chou, P. Feng and X. Bu, *Angew. Chem., Int. Ed*., 2011, **50**, 8858-8862; (*d*) J. Qian, F. Jiang, D. Yuan, M. Wu, S. Zhang, L. Zhang and M. Hong, *Chem. Commun*., 2012, **48**, 9696-9698; (*e*) H. Yang, F. Wang, Y. Kang, T.-H. Li and J. Zhang, *Dalton Trans*., 2012, **41**, 2873-2876.

10 G. M. Sheldrick, SHELXTL-97, Program for Crystal Structure Refinement, University of Gottingen, 1997.

11 V. Blatov, A. Shevchenko, V. Serezhkin, D. Korchagin, http://www.topos.ssu.samara.ru.

12 (*a*) Q. Gao, F.-L. Jiang, M.-Y. Wu, Y.-G. Huang, D.-Q. Yuan, W. Wei and M.-C. Hong, *CrystEngComm*, 2009, **11**, 918-926.; (*b*) Y. Liu, V. C. Kravtsov, D. A. Beauchamp, J. F. Eubank and M. Eddaoudi, *J. Am. Chem. Soc*., 2005, **127**, 7266-7267.

13 A. L. Spek, J. Appl. Crystallogr., 2003, **36**, 7-13.

14 M. O'Keeffe, M. A. Peskov, S. J. Ramsden and O. M. Yaghi, *Accts. Chem. Res.* 2008, **41**, 1782-1789.

15 (*a*) S.-T. Zheng, C. Mao, T. Wu, S. Lee, P. Feng and X. Bu, *J. Am. Chem. Soc*., 2012, **134**, 11936-11939; (*b*) Q.-R. Fang, G.-S. Zhu, M. Xue, J.-Y. Sun and S.-L. Qiu, *Dalton Trans.,* 2006, 2399-2402; (*c*) S. Hu, J.-P. Zhang, H.-X. Li, M.-L. Tong, X.-M. Chen and S. Kitagawa, *Cryst. Growth Des*., 2007, **7**, 2286-2289.

16 (*a*) S. Chen, J. Zhang, T. Wu, P. Feng and X. Bu, *J. Am. Chem. Soc*., 2009, **131**, 16027-16029; (*b*) Y. Liu, V. C. Kravtsov and M. Eddaoudi, *Angew. Chem., Int. Ed*., 2008, **47**, 8446-8449; (*c*) Q. Fang, G. Zhu, M. Xue, Z. Wang, J. Sun and S. Qiu, *Cryst. Growth Des*., 2007, **8**, 319-329; (*d*) T. Panda, P. Pachfule and R. Banerjee, *Chem. Commun*., 2011, **47**, 7674-7676.

17 (*a*) P.-F. Shi, G. Xiong, B. Zhao, Z.-Y. Zhang and P. Cheng, *Chem. Commun*., 2013, **49**, 2338-2340; (*b*) S. Hu, Z.-M. Zhang, Z.-S. Meng, Z.-J. Lin and M.-L. Tong, *CrystEngComm*, 2010, **12**, 4378-4385; (*c*) Q. Chen, F. Jiang, D. Yuan, L. Chen, G. Lyu and M. Hong, *Chem. Commun*., 2013, **49**, 719-721; (*d*) S. Mendiratta, M. Usman, T.-T. Luo, B.-C. Chang, S.-F. Lee, Y.-C. Lin and K.-L. Lu, *Cryst. Growth Des*., 2014, **14**, 1572-1579.

18 D.-S. Li, Y.-P. Wu, J. Zhao, J. Zhang and J. Y. Lu, *Coord. Chem. Rev*., 2014, **261**, 1-27.

19 (*a*) J.-P. Zhang and X.-M. Chen, *Chem. Commun*., 2006, 1689-1699; (*b*) B. Wang, A. P. Cote, H. Furukawa, M. O/'Keeffe and O. M. Yaghi, *Nature*, 2008, **453**, 207-211; (*c*) A. Phan, C. J. Doonan, F. J. Uribe-Romo, C. B. Knobler, M. O'Keeffe and O. M. Yaghi, *Acc. Chem. Res*., 2009, **43**, 58-67; (*d*) T. Wu, J. Zhang, C. Zhou, L. Wang, X. Bu and P. Feng, *J. Am. Chem. Soc*., 2009, **131**, 6111-6113.

20 (*a*) J. Yu, Y. Cui, C. Wu, Y. Yang, Z. Wang, M. O'Keeffe, B. Chen and G. Qian, *Angew. Chem., Int. Ed*., 2012, **51**, 10542-10545; (*b*) L. Sun, H. Xing, Z. Liang, J. Yu and R. Xu, *Chem. Commun*., 2013, **49**, 11155-11157.

21 (*a*) S.-L. Zheng, J.-H. Yang, X.-L. Yu, X.-M. Chen and W.-T. Wong, *Inorg. Chem*., 2003, **43**, 830-838; (*b*) N. B. Shustova, A. F. Cozzolino and M. Dincă, *J. Am. Chem. Soc*., 2012, **134**, 19596-19599; (*c*) J. Sahu, M. Ahmad and P. K. Bharadwaj, *Cryst. Growth Des*., 2013, **13**, 2618-2627.